

Fig. 5: The influence of noise on the behavior of NSPF with 40 W, 5 ns (T_0) super-Gaussian pulses in a 4 mm long waveguide. The red dots represent the ratio at 7% and 20% noise level.

In addition to examining the temporal profiles of the input and output pulses, we have also calculated the ratio of output to input pulse energy, R_{out} , as a function of noise level x , as shown in Fig. 5. Small values of R_{out} , corresponding to low noise level, indicate that most of the input energy of the pulse has been blocked by the output polarizer LP2, which is the result of polarization flipping in the waveguide. As x increases and R_{out} asymptotically approaches 0.5, almost half of the input pulse energy goes through the polarizer which indicates that the output pulse is fully depolarized. Figure 5 suggests that the noise level of up to 7% does not significantly affect NSPF behavior, for the specific waveguide considered in this example. Note that the typical noise level of commercial laser systems is around 5% to 10%.

5. Effects of dispersion

In our previous model of the nonlinear interaction of two polarizations [19], we ignored the temporal dependence of the pulses or dispersive effects. However, in practice, pulsed lasers are required to achieve high peak powers. In such cases, the dispersion of the waveguide becomes important and must be considered in order to correctly describe NSPF behavior. We start with Eqs. (1) and transform them into the Fourier domain to obtain:

$$\begin{aligned}
 \frac{\partial A_1(\omega)}{\partial z} &= -\frac{\alpha_1}{2}A_1(\omega) + i\beta_1(\omega)A_1(\omega) + i\left(\gamma_1|A_1(\omega)|^2 + \gamma_c|A_2(\omega)|^2\right)A_1(\omega) \\
 &\quad + i\gamma'_c A_1^*(\omega)A_2^2(\omega)\exp(-2iz\Delta\beta), \\
 \frac{\partial A_2(\omega)}{\partial z} &= -\frac{\alpha_2}{2}A_2(\omega) + i\beta_2(\omega)A_2(\omega) + i\left(\gamma_2|A_2(\omega)|^2 + \gamma_c|A_1(\omega)|^2\right)A_2(\omega) \\
 &\quad + i\gamma'_c A_2^*(\omega)A_1^2(\omega)\exp(2iz\Delta\beta),
 \end{aligned} \tag{12}$$

where $\beta_n(\omega)$ $n = 1, 2$ are the propagation constants of the fundamental modes of the waveguide at the frequency ω , $\Delta\beta = \beta_1(\omega_0) - \beta_2(\omega_0)$ and ω_0 is the central frequency of the input pulse which in this case is $\omega_0 = 2\pi c/\lambda_0$ where c is the speed of light and $\lambda_0 = 1550$ nm. The advantage of writing the coupled nonlinear Schrödinger equations in the frequency domain, as in Eqs. (12), is that $\beta_1(\omega)$ and $\beta_2(\omega)$ include the full dispersion of the two polarizations rather than only a few dispersion orders (as in Eq. (1)). We have solved Eqs. (12) numerically, using a Fourier split step method, for the waveguide shown in Fig. 1. The propagation constants of the waveguide are calculated by using a finite element package (COMSOL). For this waveguide, the group velocity dispersion of both polarizations are anomalous at the pump wavelength. To

confirm the validity of our numerical model, we have first considered the results of the numerical model for quasi-CW pulses, with a very narrow line width, and confirm that they match the analytical results of the CW model in [19], see Fig. 4 (a).

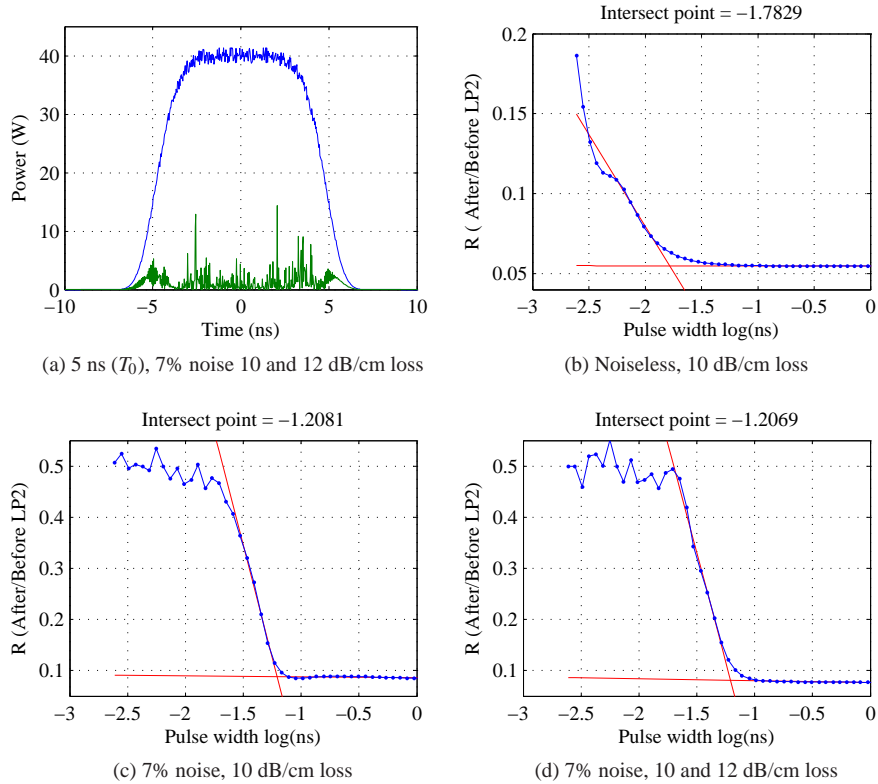


Fig. 6: The influence of dispersion on the behavior of NSPF. (b-d): The intersections of the red lines define the threshold of pulse width for each case.

The influence of dispersion on NSPF cannot be isolated from that of other parameters such as the noise. Figures 6(b) and 6(c) show the ratio of the input to output pulse energies, R_{out} , as a function of pulsewidth [$\log_{10}(\text{pulsewidth})$] for waveguides with and without laser noise. In both figures, for longer pulses R_{out} approaches an asymptotic value. As the pulsewidth decreases, R_{out} increases quickly indicating that the output pulses are depolarized. We define the intersection between the asymptotic values of R_{out} and a line representing the fast growing section of R_{out} graph (red lines in Figs. 6(b)–6(d)), as the minimum pulsewidth for which NSPF behavior is still observed. It is observed that NSPF behavior can be observed for pulsewidths as low as 16.5 ps for the noiseless case, Fig. 6(b). However, the minimum pulsewidth for which NSPF behavior can be observed, when a noise level of 7% is considered, is of order 62 ps. This can be explained by noticing that the noise in our model is broadband and acts as a seed of some spontaneous nonlinear processes such as four-wave mixing and modulation instability. Figure 6 (d), shows R_{out} as a function of pulsewidth when the loss of the two polarizations are different, 10 and 12 dB/cm. In this case, the minimum pulsewidth is similar to Fig. 6(c) for which the two polarizations have the same loss of 10 dB/cm.

6. Conclusion

We have shown the feasibility of achieving NSPF in fabricable silicon waveguides by investigating the behavior of NSPF in a silicon waveguide with realistic parameters. We have studied the combined effects of structural variation, waveguide loss, laser noise and waveguide group velocity dispersion on NSPF. For every parameter, we have determined the range for which NSPF can be observed. We have shown that NSPF should be observed in a 400 nm silicon waveguide using tunable pulsed lasers with pulse widths bigger than 62 ps, laser noise level lower than 7%, loss of 10 dB/cm and peak power of a few tens of watts.

The study here focused on a typical silicon waveguide structure, shown in Fig. 1, and hence the parameter ranges, for which NSPF can be observed, are specific to the particular waveguide and setup used in this study. The range of these parameters change for other waveguide structures. It would be possible to identify the waveguide structure that optimizes one or more of these parameters.

One important parameter that affects NSPF behavior is the dispersion which is determined by the waveguide geometry (refractive index distribution $n(x,y)$). There may be an optimum dispersion profile for NSPF behavior. However, to investigate this possibility as well as to discover other interesting nonlinear effects, further development of the original full vectorial nonlinear Schrödinger equations is required. Such equations should describe the nonlinear interaction of the two polarizations, to include temporal effects (dispersion), which by itself is a topic for future investigation.

The study here shows that typical silicon waveguides with structures shown in Fig. 1 and with practical parameters can be used for nonlinear polarization switching.

Acknowledgments

We acknowledge the support of the South Australia State Government and the Italian Regional Government for funding this work. Authors Zhang, Lohe, Monroe, and Afshar V. also acknowledge ARC funding support (DP110104247). Tanya Monroe also acknowledges the support of a Federation Fellowship.